Electron momentum spectroscopy and linear combination of atomic orbitals calculation of bulk Na_2O

2003 J. Phys.: Condens. Matter 15 2155

(http://iopscience.iop.org/0953-8984/15/13/302)

INSTITUTE OF PHYSICS PUBLISHING JOURNAL OF PHYSICS: CONDENSED MATTER

J. Phys.: Condens. Matter **15** (2003) 2155–2168 PII: S0953-8984(03)58709-4

Electron momentum spectroscopy and linear combination of atomic orbitals calculation of bulk Na_2O

E A Mikajlo[1], K L Nixon[1] and M J Ford[2]

[1] School of Chemistry, Physics and Earth Science, Flinders University, GPO Box 2100, SA 5001, Australia
[2] Institute for Nanoscale Technology, University of Technology, Sydney, PO Box 123, Broadway NSW 2007, Australia

E-mail: mike.ford@uts.edu.au

Received 23 January 2003
Published 24 March 2003
Online at stacks.iop.org/JPhysCM/15/2155

Abstract

This paper presents an experimental measurement of the electronic structure of Na_2O in the solid phase using electron momentum spectroscopy and compares the results with *ab initio* calculations performed within the linear combination of atomic orbitals (LCAO) approximation. While Hartree–Fock (HF) can reproduce elastic properties we find it overestimates splitting of the oxygen valence bands by around 30% and the width of the O 2p band by a factor of 2. Our experimental values are 15.85 ± 0.2 and 0.6 ± 0.2 eV for these two quantities, respectively. Density functional methods are significantly better, with the hybrid functional PBE0 predicting the oxygen bandgap to within the experimental error. PBE0 also gives the best estimate of the Na core level energies. In contrast, HF performs best for the splitting between the oxygen and sodium bands. Our experimental values of 32.85 ± 0.2 and 27.45 ± 0.2 eV for the Na 2p–Na 2s and O 2p–Na 2p splittings agree well with previous measurements. Distribution of electron density both within the bands and between the bands is not reproduced by any of the computational methods employed.

1. Introduction

Sodium oxide (Na_2O), like the other alkali oxides, crystallizes into the anti-fluorite structure with 30 electrons in the unit cell. It is this relative simplicity in structure and small electron count that make it an ideal candidate for computational studies at the *ab initio* level. Furthermore, it is a rather prototypical ionic solid that provides a benchmark for assessing the performance of theoretical models, and is the starting point for studies of more complex transition metal oxides.

At the core of any *ab initio* quantum chemical method is a calculation of the electronic structure, from which other physical and chemical properties are, in a sense, derived. Despite this, there are few comparisons of experimental electronic structures with theoretical predictions to be found in the literature for any of the simple oxides. To date, calculations have largely been assessed on their ability to reproduce lattice parameters, elastic constants and other structural parameters. Very few experiments to determine the electronic structure of Na_2O have been made so far, probably due to its highly insulating nature and the associated difficulties with sample charging.

Electron momentum spectroscopy (EMS) complements established condensed phase techniques for measuring electronic structure, such as photoemission spectroscopy. It provides a very direct measurement of electron motion requiring no theoretical input for its analysis, can be applied equally to crystalline, polycrystalline and amorphous samples and, as we have previously demonstrated, can provide band structure measurements of insulating solids [1–3].

In the present work we attempt to bridge the gap in experimental data and provide a complete mapping of the band dispersions and band intensities for bulk Na_2O using the EMS technique. We compare our experiments with tight binding calculations performed with the CRYSTAL98 software package [4]. The experimental and theoretical results complement existing studies and reveal aspects of the theoretical models that are not apparent from previous structural studies alone [5]. Comparison of theory and experiment in the present work also provides a valuable guide to development and characterization of the EMS technique itself.

Early Auger and x-ray photoelectron spectroscopic studies of both sodium metal and sodium oxide were performed in 1975 by Barrie and Street [6]. Using Mg Kα radiation (1254 eV) the authors report binding energies and linewidths for all of the sodium levels relative to the Na 1s level. A more recent x-ray photoelectron study by Shek *et al* [7] in 1991 focuses on the early stages of oxidation of sodium by measuring the Na 2p and valence band photoemission data of sodium thin films. Compton scattering, which provides a very detailed picture of the electron momentum density (EMD) of the target integrated over binding energy, has been applied to metallic sodium and sodium halides [8], but we find no reports of this technique being applied to the oxide. Likewise, to our knowledge, angle-resolved photoemission spectroscopy (ARPES), capable of mapping the occupied band structure of crystalline solids, has yet to be applied to this simple system.

The theoretical study published by Dovesi *et al* in 1991 [5] applied an earlier version of the CRYSTAL code [9] to investigate the elastic properties of the lighter alkali oxides at the Hartree–Fock (HF) level. While reasonable agreement was found with experimental lattice parameters and elastic constants for Na_2O, binding energies differed by more than 40% due to the lack of correlation. Electronic structures were not investigated. We extend this study in the present work to include density functional (DFT) methods and calculation of the electronic structure as well as physical structure and energetics.

Having provided the background and motivation for the present work, in the next two sections we outline the experimental and computational methods employed, followed by a detailed analysis, discussion and comparison of experiment and theory in section 4 and concluding remarks in the final section.

2. Experiment

Electron momentum, or (e, 2e), spectroscopy will not be described here; there are a number of excellent reviews of the technique [10] and its application to the condensed phase [11] in the literature. The spectrometer used in the current work is also described in detail elsewhere [12, 13]. Suffice it to say that EMS is a medium energy (20 keV) electron beam

technique which relies upon ionization of the target and subsequent energy and angle selection of the outgoing electrons. It is a transmission technique and the solid target must be prepared in the form of an ultra-thin, free-standing membrane in order to minimize multiple scattering [14]. The critical point is that the electron density within the target as a function of real (not crystal) momentum *and* binding energy is measured directly. EMS gives the band structure (or band dispersions) together with the distribution of electrons within each band for almost any target that can be prepared as a sufficiently thin film, whether it is a crystalline film with well defined stoichiometry, or a complex amorphous structure of varying composition. However, target preparation is the central issue facing EMS.

In our spectrometer data can be collected over a 70 eV energy window within a single experiment. This allows simultaneous measurement of the oxygen valence bands and metallic core levels of the group I oxides [2]. The overall energy and momentum resolution of our spectrometer is around 1 eV and 0.1 atomic units, respectively. Data require around 100 h of continuous measurement in order to build up sufficient statistics. Relatively small beam currents, of the order of 100 nA, are used. The total electron irradiation dose in the EMS experiment is therefore comparable with standard characterization measurements such as Auger spectroscopy [15], despite the difference in data collection rates.

Our Na_2O films are prepared by thermally evaporating sodium (99.95% purity) onto a 3 nm thick amorphous carbon substrate in the presence of an oxygen background at 5×10^{-7} Torr; background pressure in this evaporation chamber is around 10^{-10} Torr. An evaporation rate of 0.02 nm s^{-1} was used. Under these conditions the flux of sodium atoms arriving at the am-C substrate is much larger than for oxygen and we might reasonably expect Na_2O to form together with some un-oxidized metal [16]. Furthermore, our EMS spectra show a single broad O 2p feature characteristic of oxygen being present as the atomic species in the oxide, rather than as molecular oxygen [16, 17]. However, the EMS data showed no sign of a free-electron parabola associated with the presence of metallic sodium. Samples prepared in this manner are expected to be polycrystalline. The spectrometer is relatively surface sensitive, with the EMS signal originating in the outermost 2 nm of the target, while the remainder of the target contributes only to the multiple scattering background in the data. Sample preparation is then a trade-off between a thick enough oxide overlayer such that the carbon is sufficiently covered and does not contribute to the true EMS signal, but thin enough that multiple scattering does not dominate.

A series of samples were prepared with varying oxide thickness, the deposited thickness being monitored by a quartz crystal microbalance. If the evaporated layer was less than 8 nm thick, the amorphous carbon substrate was evident in both Auger and EMS spectra. An oxide layer of 9.5 nm initially showed no carbon in the EMS spectrum. After about three hours, electronic bands due to carbon begin to appear and become more dominant as the measurement progresses. We suspect that the carbon substrate is only just covered and the electron beam causes the overlayer to island, leaving large areas of exposed carbon. Increasing the thickness to 16 nm provided the best compromise between the effect of increased multiple scattering and contamination of the Na_2O results with carbon.

Figure 1 shows typical Auger spectra for a 16 nm sample. The Auger spectrum of the sample taken immediately after evaporation shows peaks corresponding to both O and Na KLL transitions and there is no clear indication of the presence of carbon at the sample surface. A carbon KLL transition has appeared in the Auger spectrum of figure 1(c) taken after 22 h of EMS measurement. No change was detected in the EMS band structure over this time period, but EMS is less surface sensitive than Auger spectroscopy. The final EMS data was obtained by adding together a series of identical samples, each one measured for less than 20 h. No evidence of sample charging is found in the EMS data and the binding energy peaks are

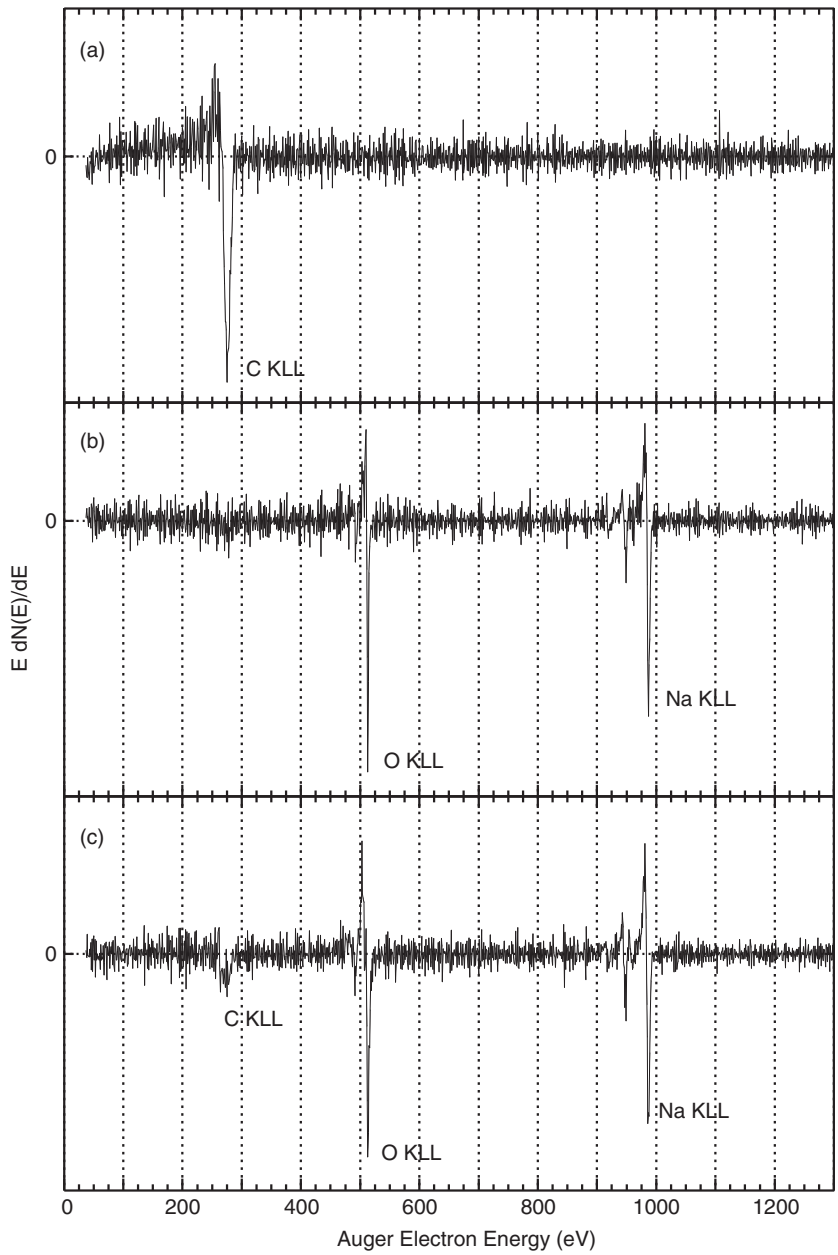

Figure 1. Differential Auger spectrum of the target (a) prior to evaporation, (b) immediately after evaporation and (c) after 22 h exposure to the EMS electron beam.

entirely stable in energy over the course of the measurement. This is perhaps surprising given that Na_2O is a good insulator, but is consistent with our findings for other oxides. Either the carbon substrate allows charge to 'leak' out of the oxide layer, or charging is relatively weak and occurs rapidly, thereafter stabilizing for the remainder of the measurement.

Our EMS data for Na_2O are shown in figure 2. We present the result here simply to point out that this is the direct output of the experiment and to provide a guide to interpreting this

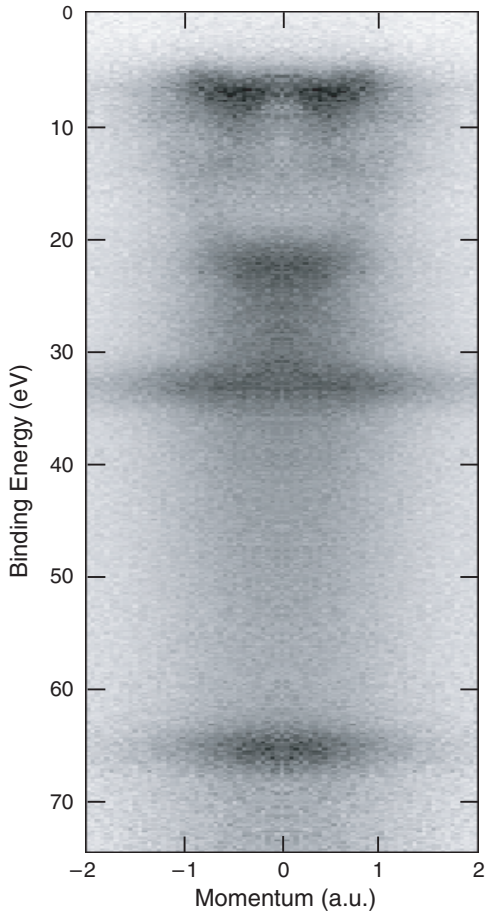

Figure 2. Experimental EMS data. Binding energy is relative to the vacuum level of the spectrometer, electron momentum is in atomic units. Electron density is represented on a linear grey scale with darker colours representing higher density.

data. The y axis, or binding energy of the electrons in the target, is relative to the vacuum level of the spectrometer, that is the work function of the sample plus any contact potentials present in the electron gun and analysers, plus in principle any charging effects in the target. For this reason we compare only relative energies with calculated results or other experiments. The x axis is the *real* momentum of the electrons in the target: the data are necessarily symmetric about zero momentum. The z axis is a grey scale representing electron density, darker colours signifying higher occupation. Overall, figure 2 is analogous to the familiar band structure plots found in most solid state physics texts (see, for example, [18, p 215]). The latter represents band dispersions, both occupied and unoccupied, plotted as a function of the binding energy (relative to the Fermi energy) and wavevector (or crystal momentum). They are often plotted in terms of the high symmetry points of the reciprocal lattice, rather than wavevector directly, and are generally in the reduced zone scheme. EMD plots show how the electrons are distributed within a given band(s). Figure 2 gives the band dispersions, occupied bands only, and EMDs convoluted together into a single plot, represented effectively in the extended zone scheme. Our samples are expected to be polycrystalline and so our EMS data are a spherical average over all crystal directions. We will return to an analysis and discussion of these results in section 4.

3. Calculations

The electronic structure calculations were performed using the commercially available software package CRYSTAL98 [4] which performs *ab initio* calculations of the ground state wavefunction and properties of periodic systems. The single-particle wavefunctions, or crystalline orbitals, are approximated as a linear combination of Bloch functions defined in terms of local or atomic orbitals: the linear combination of atomic orbitals (LCAO) approximation. The electronic structure of Na_2O was calculated using HF and three DFT Hamiltonians. The functionals employed were Dirac–Slater exchange [19] with Vosko–Wilk–Nusair correlation [20] to represent the local density approximation (LDA), Perdew–Burke–Ernzerhof exchange and correlation [21] for the generalized gradient approximation (PBE) and PBE exchange and correlation mixed with 25% exact HF exchange [22] for the hybrid functional (PBE0).

High quality all-electron basis sets were used. They are recommended by the authors of CRYSTAL98 and have previously been optimized at the HF level. These are an 8-511G contraction on the sodium ion and a 8-411G contraction on the oxygen ion. Dovesi *et al* [5] have shown that these relatively small basis sets give reliable results and that the addition of polarization functions or a second valence shell has only minor effects on the predicted elastic properties of Na_2O. We would expect the basis set effects to be minor in the case of electronic structure also and below the level of detection in our experiment [23].

All the calculations were performed at the default tolerances for the CRYSTAL98 package and sampled at 28 points within the irreducible wedge of the Brillouin zone. The characteristic anti-fluorite crystal structure for sodium oxide was used with a lattice parameter of 0.549 nm. This is the athermal limit to the experimental lattice parameter (0.555 nm) [5]. The k-point sampling and tolerances employed are sufficient to give converged electronic structures, at least at the level of our experimental accuracy. Strictly speaking, it is more appropriate to use the optimum lattice constant in each calculation rather than the experimental value. This is true for binding energies. However, as we have already demonstrated [2] the difference is minor and can be neglected in the case of electronic structures.

The calculated band dispersions and EMDs along three high symmetry directions for the HF calculation are given in figure 3. The three DFT methods give band structures that are qualitatively similar, albeit with different binding energies and bandwidths. Our optimum lattice parameters together with Γ-point energies relative to the valence band maximum and bandwidths for all four theoretical methods are given in table 1.

Our optimized lattice constant at the HF level agrees well with the earlier calculation of Dovesi *et al* [5]: the small difference can be ascribed to different computational conditions. It also agrees very well with the experimental value, extrapolated to the athermal limit, of 0.549 nm. Amongst the DFT methods, LDA underestimates, GGA overestimates and inclusion of exact exchange gives essentially the same result as HF.

The Γ point energies and bandwidths are similar for all three DFT methods and significantly smaller than the HF calculations. The sodium-derived bands show no dispersion as would be expected for these core-like levels.

4. Analysis and discussion

Returning to the experimental EMS results of figure 2, this spectrum is typical for the electronic structure of an ionic solid where there are a number of bands separated by large energy gaps. Four bands are present, at about 7, 23, 34 and 66 eV relative to the vacuum level. From the top downwards they are derived from the oxygen 2p, oxygen 2s, sodium 2p and sodium 2s

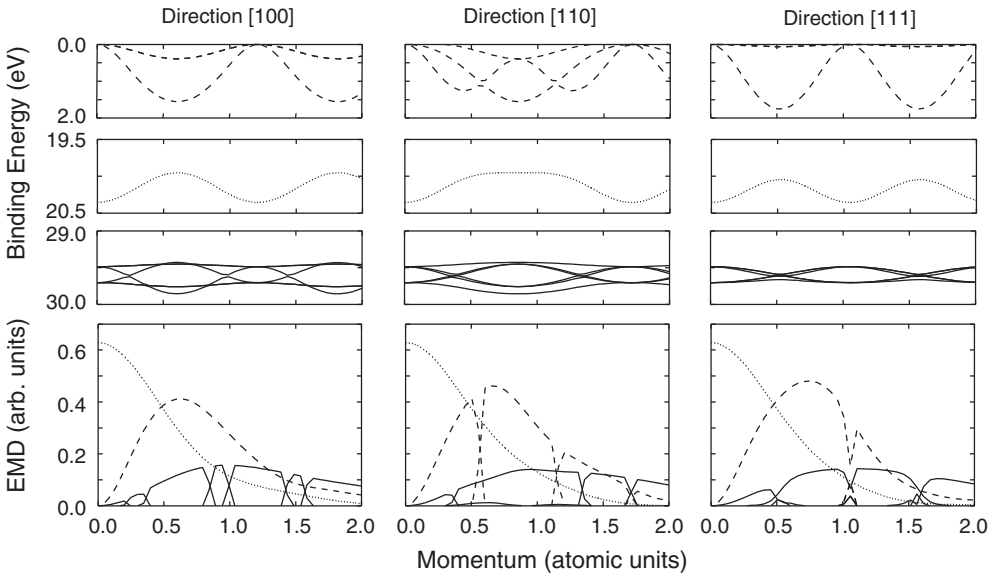

Figure 3. HF band dispersions and EMDs calculated along three high symmetry directions. Binding energies are relative to the valence band maximum.

Table 1. Optimized lattice parameters (nm), Γ point binding energies (eV) relative to the valence band maximum and bandwidths (eV).

Method	HF	LDA	PBE	PBE0
a_0	0.5497	0.5393	0.5559	0.5498
O 2p	0	0	0	0
ΔE O 2p	1.77	1.51	1.45	1.59
O 2s	20.22	14.23	14.53	16.02
ΔE O 2s	0.40	0.33	0.31	0.34
Na 2p	29.33	21.60	21.83	23.75
Na 2s	64.22	49.00	49.83	53.52

orbitals, respectively. Na_2O is quite ionic and so one expects that there is little contribution from metallic sodium orbitals to the predominantly oxygen valence band and this simple assignment of the bands to orbitals located either on the anion or cation is quite reasonable. Overlap between orbitals situated on neighbouring ions decreases going down figure 2, as evidenced by the decreasing bandwidths, or dispersions. The core-like sodium levels are very atomic-like, showing no dispersion. Within the O and Na 2s bands, maximum electron density occurs at the Γ point, i.e. zero momentum, whereas it is away from this point for the 2p bands. This is consistent with the momentum distributions for atomic 2p and 2s orbitals.

Apart from the bands described above, additional intensity is present in figure 2 due to multiple scattering of the (e, 2e) electrons within the target. Multiple scattering can take the form of inelastic processes, such as plasmon or valence excitation, and small angle elastic scattering. Collective plasmon oscillations do not appear to significantly affect the EMS spectrum for Na_2O. Using photoelectron spectroscopy Barrie and Street determined the first two plasmon energies to be 6.5 ± 0.2 and 13.2 ± 0.3 eV [6]. However, the peaks are broad and indistinct and unlikely to be strong enough to produce peak-like features in our EMS spectrum.

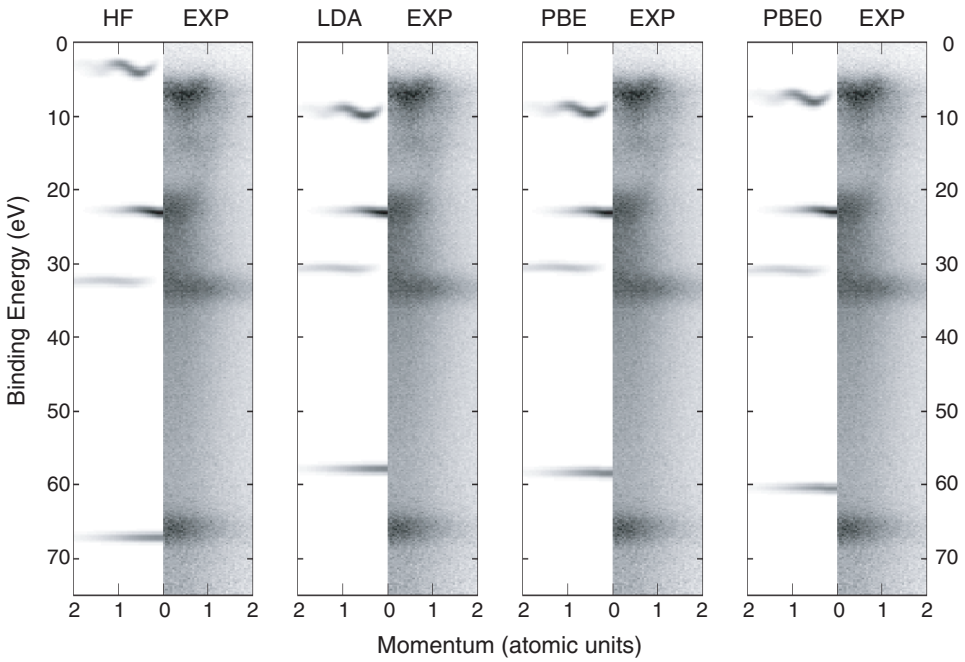

Figure 4. Comparison of experimental and calculated energy and momentum resolved electron densities. Experimental data are identical in every panel. Binding energy is relative to the vacuum level of the spectrometer and calculated energies have been normalized to the experiment at the Γ point of the O 2s band.

Overall, the multiple scattering background is much less evident than in our measurements of metallic [15] or semiconducting targets [24].

Despite attempts to minimize carbon contamination, a faint parabolic structure is also evident in figure 2 with its minimum between the O 2s and the Na 2p bands extending towards the higher momentum edge of the O 2p band. The shape and position of this feature, together with the emergence of a carbon signal in the Auger spectrum after being subjected to the (e, 2e) beam, suggest that it is due to the σ-valence band in amorphous carbon [25].

To compare our theory directly with experiment we fold the EMDs into the band dispersions of figure 3 to produce a single energy and momentum resolved electron density plot. In addition we spherically average the theory by performing calculations along a number (in our case 25) of evenly spaced directions within the irreducible wedge of the Brillouin zone and summing the results together [23]. Finally the calculated spectra are convoluted with Gaussians of 1 eV and 0.1 au to account for the experimental resolutions. The results of this process for all four calculations alongside the experimental data are shown in figure 4.

Qualitatively the calculations provide a good prediction of the measured band structure. Obviously, the calculated spectra contain no multiple scattering background. HF appears to give the best overall agreement, except for the valence band where it drastically overestimates the splitting between the oxygen bands. The DFT methods fair much better in this regard, particularly PBE0, but do not give an adequate prediction of the core level energies, particularly the O 2s–Na 2p gap.

The data of figure 4 need to be presented in a different format in order for a quantitative comparison to be made. We take vertical slices, with a momentum width of 0.1 au through

Table 2. Bandgaps measured at the Γ point for the experimental data and the spherically averaged theoretical predictions. The error in experimental values is ±0.2 eV.

	EXP	HF	LDA	PBE	PBE0
O 2p–O 2s	15.85	20.22	14.23	14.53	16.02
Na 2p–Na 2s	31.49	34.90	27.40	28.00	29.77
O 2s–Na 2p	11.74	9.11	7.37	7.30	7.73
ΔE O 2p	0.60	1.22	1.01	0.96	1.07

the plots in figure 4, to produce a series of binding energy spectra. In addition, a fourth-order polynomial is used to subtract the background in these spectra. The results for the experiment and the PBE0 calculation are shown in figure 5 (for clarity not all the momentum slices are shown). The observed O 2p binding energy peak is a broad feature with a small shoulder on the high binding energy side. This is indicative of the presence of Na_2O: the peroxide (or indeed superoxide) would give a series of peaks spread over about 10 eV [16, 17]. The small shoulder on the side of the peak could indicate a small amount of the peroxide is present, but is more likely due to multiple scattering or the am-C substrate.

To provide a convenient summary of all our data that are readily compared with other results we have extracted peak positions and peak areas from all four calculated and experimental binding energy spectra similar to figure 5. A least squares fitting procedure was used to fit Gaussians to the binding energy peaks. It is clear from figure 5 that the peaks are not always described by a single Gaussian; the high energy shoulder on the O 2p peak, for example. These were taken care of by fitting an additional Gaussian. The quality of the fits is extremely good, except at higher momentum values in the experimental data where peak intensities are relatively small. Γ point bandgaps and O 2p bandwidths derived from the fits are given in table 2. Bandgaps are calculated from the energy difference in peak position of the fitted Gaussians at the Γ point and bandwidths from the energy difference of the band maximum and minimum. Other bandwidths are too small to be determined reliably by this method. The full band dispersion and EMD for the O 2p band is shown in figure 6. The errors in the data have been estimated from the fitting procedure and take into account the statistical errors present in the binding energy spectra.

4.1. Band intensities

Looking at figure 5 it is clear that intensities are not well reproduced by the PBE0 calculation. Most striking is the large intensity at the Γ point in the oxygen and sodium p bands seen in the experiment whereas in the calculation it is virtually zero. The other three calculations make essentially the same prediction as can be seen in the EMDs of figure 6.

The anomalous Γ point intensity in the p bands is, in part, due to small-angle elastic scattering redistributing intensity within the band. It is hard to see how this mechanism can produce such a dramatic effect, however. In the case of BeO we have made an initial attempt to assess this effect by simulating multiple scattering in the calculation [23]. The results still produce only a small O 2p peak compared with the 2s peak at zero momentum. The finite momentum, or angular resolution, of the spectrometer will also smear intensity along the momentum axis. Measurements with the current spectrometer on the 3p state of atomic argon, where the intensity is known to be zero at zero momentum, have been performed by Storer *et al* [12]. The results show the effect of finite resolution giving non-zero intensity at zero momentum, but not to the extent observed in our Na_2O measurement. In any case, we have taken account of this by convoluting the calculation with a Gaussian of momentum width

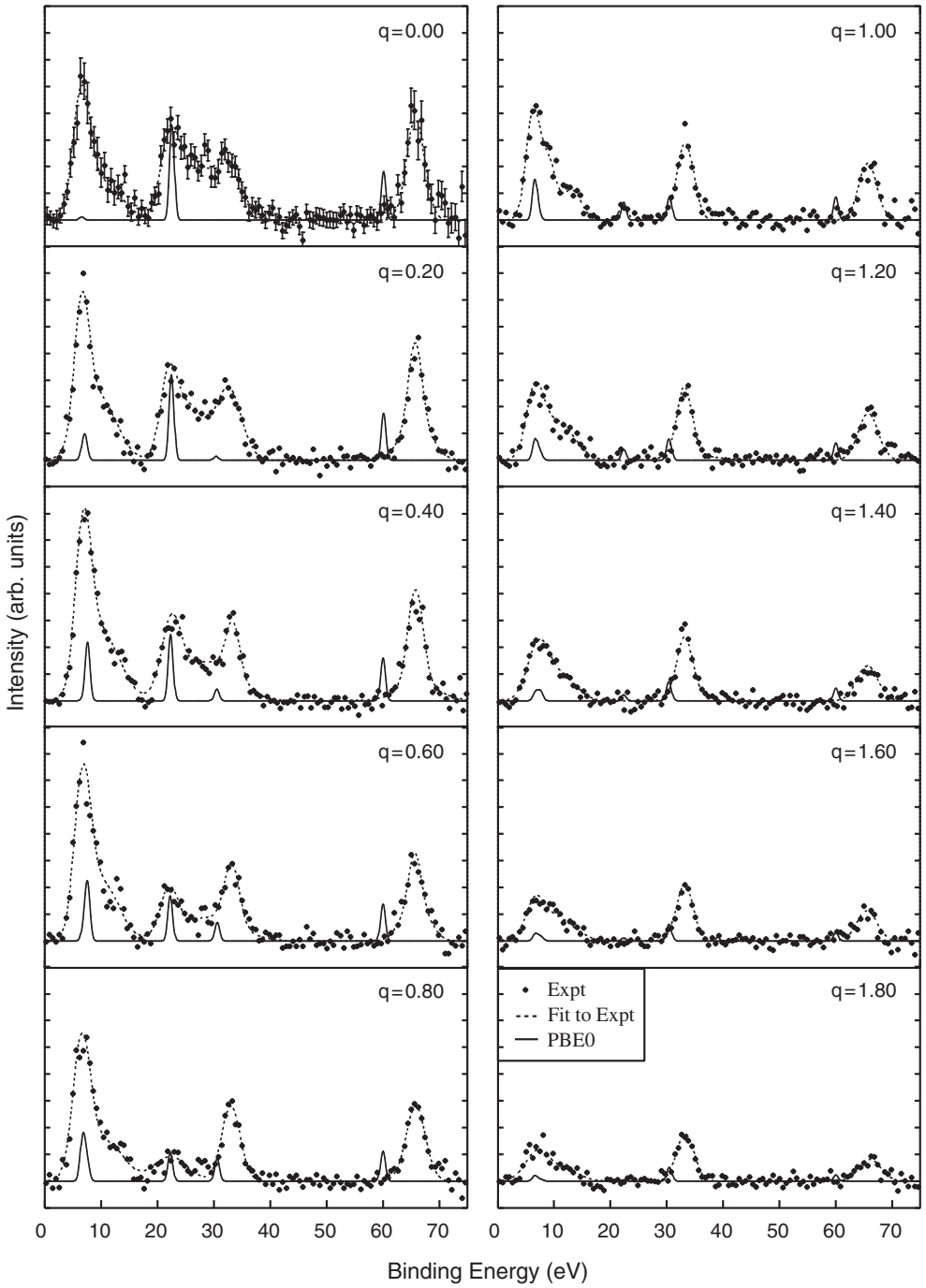

Figure 5. Experimental and calculated binding energy profiles extracted from figure 4 by integrating over 0.1 au intervals. Binding energies are relative to the vacuum level of the spectrometer. Calculated binding energies and intensities have been normalized to the experiment for the O 2s peak in the 0 au momentum interval.

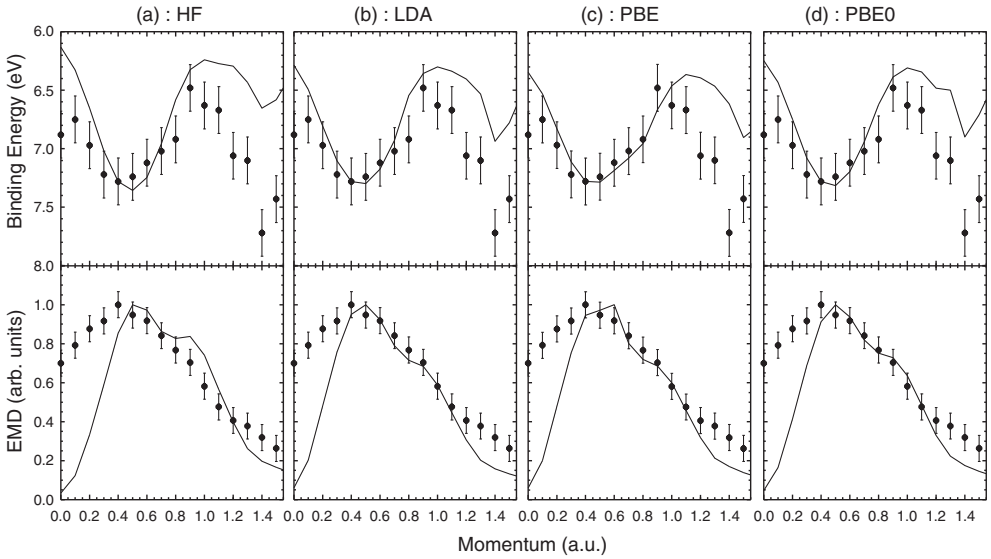

Figure 6. Band dispersion (upper panel) and EMDs (lower panel) extracted from the binding energy profiles of figure 5. Binding energies are relative to the vacuum level of the spectrometer. Experimental and calculated band dispersions have been normalized at the band minimum, EMDs have been normalized at the maximum. Points with error bars are experimental data and full curves are the calculations.

0.1 au. Storer *et al* [12] derive a resolution of 0.15 au in their experiment, the performance of the spectrometer has since been improved with the addition of a monochromator on the electron beam and the resolution is estimated to be around 0.1 au [13]. Convoluting the calculation with a momentum width of 1.0 au still only produces an O 2p peak that is about one quarter the height of the O 2s peak. The same arguments can be made for the energy resolution.

The same phenomenon is observed in our measurement for Li_2O and the three lighter group II oxides, suggesting a systematic cause. The use of different Hamiltonians has little effect in the calculations, and it is unlikely that basis set effects can be singled out. In fact, calculations using other approaches, such as plane-wave codes, do not provide an explanation either. If the problem lies in the model then it is more likely our description of the sample that needs to be improved. In addition, there may be other instrumental factors, such as sensitivities, that we would not expect from our experience with gas phase EMS that are also playing a role.

Relative intensities of the bands are not reproduced by any of the calculations. Most noticeably the ratio between the O 2s band and any of the other three bands is extremely poor. For example, at a momentum of 0.6 au the O 2p and 2s bands are predicted to have the same intensity, whereas we observe a factor of 2 difference. It is hard to see how multiple scattering and resolution effects could redistribute intensity *between* the bands. The explanation that solid state EMS does not have equal sensitivity to all the bands is attractive in this case, but we cannot rule out possible problems with the model employed in the calculations. Above about 0.4 au momentum the relative intensities of the O 2p, Na 2p and Na 2s bands are reasonably well predicted.

The widths of the binding energy peaks in figure 5 are also not reproduced by the calculations. The overall energy resolution of the spectrometer has been measured by Canney *et al* to be 1 eV (FWHM) [13] and our calculations are convoluted with the corresponding Gaussians. Looking at the Na 2s core level, the experimental resolution would have to be around

5 eV to produce a peak of this width. Multiple scattering, in particular small-angle elastic scattering which smears intensity along the momentum axis, makes a significant contribution to this observed width, as we have found in our analysis of BeO [23]. Electron–hole lifetime effects [26] and thermal broadening can also contribute to the overall peak width.

4.2. Band energies

Turning to the Γ point bandgap data in table 2 we see that HF overestimates the splitting of the oxygen valence bands by about 30%. The inclusion of correlation in the DFT methods gives smaller bandgaps that are all within about 10% of the observed value. LDA gives the smallest splitting, gradient corrections broaden the bandgap slightly and inclusion of exact exchange broadens it further, giving a result that agrees with experiment to within the error.

The trend is similar for the sodium 2p–2s splitting in that HF overestimates and all three DFT calculations underestimate. PBE0 underestimates by about 5%, HF overestimates by about 10% and the LDA and PBE functionals this time perform marginally worse than HF, underestimating by about 13 and 11%, respectively.

For the gap between the lower oxygen and upper sodium band the situation is rather different. While the order of the four calculations is preserved they all underestimate. Consequently, HF gives the best result, being about 22% away from the experimental value. The same observation was made for the O 2s–Li 1s bandgap in Li_2O [2]. In CaO we were also able to measure two cation and two anion bands but found that DFT performed best for the oxygen bandgap, calcium bandgap *and* oxygen–calcium bandgap.

The O 2p bandwidth is overestimated by about a factor of 2 at the HF level. DFT bandwidths are smaller but still broader than experiment by more than the experimental error. This is a common finding in all our previous group I [2] and II oxides [3] data, but runs contrary to conventional wisdom where HF overestimates and DFT underestimates. Our data are considerably narrower than other experimental and theoretical studies. We have already noted that caution should be exercised in comparing experimental and theoretical bandwidths [2]. However, the bandwidths in table 2 are derived in the same way from data sets that are treated essentially the same, and a direct comparison should therefore be reliable.

The overall shape of the O 2p band dispersion shown in figure 6 is reproduced by the DFT calculations. The three functionals employed give very similar results and it is difficult to choose among them on the grounds of predicted bandwidths or dispersion curves.

Calculated band energies, bandwidths and band dispersions have also been presented in table 1 and figure 3. Figure 3 gives band dispersions calculated along three definite crystal directions, and the data in table 1 are derived from these dispersion curves. The bands are degenerate at the Γ point so that a calculation along any direction will yield the same Γ point energies. That is, the bandgaps are immune to spherical averaging and bandgaps in table 1 are the same as those in table 2. However, bandwidths vary depending upon the crystal direction, and bandwidths in table 1 are calculated from band extrema along the [111] direction where the bands are widest. The data in table 2, on the other hand, are extracted from the spherically averaged calculations and bandwidths are consequently around 0.5 eV narrower. Hence, it is straightforward to compare bandgaps in this work with previously published results, but not so trivial to compare bandwidths.

The photoemission data of Barrie and Street [6] gives a value for the Na 2p–2s bandgap of 32.85 eV, in good agreement with our experimental value. Shek *et al* [7] have measured the O 2p–Na 2p bandgap with photoemission and report a value of 27.45 ± 0.2 eV, which agrees to within error with our value of 27.59 ± 0.2 eV. There are no previous measurements of the oxygen valence bandgap or theoretical reports to compare with our data.

5. Conclusion

The electronic structure of the outermost oxygen and sodium bands in Na_2O is reported in the present paper. Experiments have been performed using EMS. This technique measures directly the energy and momentum resolved electron density of the target, providing the band dispersions together with band occupation. The experiment is compared with *ab initio* calculations performed within the LCAO approximation. HF and DFT Hamiltonians are used together with high quality all-electron basis sets. The calculations are spherically averaged to account for the polycrystalline structure of the sample and convoluted with the experimental resolutions.

While HF calculations can reproduce structural properties, such as lattice parameters and elastic constants of Na_2O (and other oxides), very well they do not reproduce the electronic structure. The oxygen 2p–2s and sodium 2p–2s bandgaps are overestimated by about 30%. The difference between experiment and theory cannot easily be attributed to systematic errors in the experiment and our values agree very well with available previous experiments. It is unlikely that basis set effects are responsible either since they are complete enough that the electronic structure is relatively insensitive to increases in the basis set size. The problem most likely lies with the Hamiltonian. The use of DFT produces 2p–2s bandgaps that are consistent with experiment. The hybrid functional PBE0 incorporating 25% exact exchange gives the best agreement. However, DFT does not perform well for the gap between bands associated with different ions, that is the O 2s–Na 2p bandgap. In this case HF does best but still gives a value substantially smaller than experiment. The origin of this is unclear, but a similar result has been observed for Li_2O.

None of the calculations reproduce the O 2p bandwidth very successfully. Contrary to conventional wisdom we observe an experimental width that is smaller than both HF and DFT. Similarly, there are marked differences between the experimental and predicted band intensities. There is considerable intensity in the O 2p band at the Γ point, more than in the 2s band. The calculation, as might be expected for a band derived from p orbitals, gives essentially zero intensity even with the inclusion of the experimental resolution and spherical averaging. Also the ratio of intensities between the bands is not predicted by any of the calculations. Multiple scattering plays some role in this, although it is difficult to account for such dramatic differences with this mechanism alone. If the problem lies in the calculations then it is most likely an inadequate description of the experimental sample, which is a relatively thin layer. If the problem is instrumental then it is something particular to the application of EMS to solid targets. Non-uniform sensitivity to electrons in different bands could be a candidate in this regard. However, we cannot rule out basic inadequacies in the theory for describing ionic systems.

Comparison between experimental spectra and DFT calculations are complicated by the fact that, strictly speaking, DFT only predicts the total ground state energy and electron density. However, there is growing empirical evidence to suggest that DFT can predict single-particle energies reliably and there are numerous comparisons in the literature. In addition, we cannot absolutely rule out the possibility that our sample contains sodium peroxide despite the preparation conditions employed and the fact that the observed oxygen valence band spectrum is more consistent with Na_2O than Na_2O_2.

Some progress has already been made in simulating multiple scattering in the calculations, at least for BeO, and strengthens our claim that this mechanism cannot explain the discrepancies in the intensities. In the future we intend to perform calculations where the target is modelled more realistically by performing slab calculations rather than bulk.

Acknowledgments

This work was supported by the Australian Research Council, Flinders University, and the University of Technology, Sydney. EAM and KLN were supported by SENRAC and Ferry scholarships, respectively. The authors gratefully acknowledge workshop staff and facilities at Flinders University. Calculations were performed on the Chemistry Computing Cluster at Adelaide University.

References

[1] Ford M J, Dorsett H E and Brunger M J 2001 *Trends Appl. Spectrosc.* **3** 145
[2] Mikajlo E A, Nixon K L, Coleman V A and Ford M J 2002 *J. Phys.: Condens. Matter* **14** 3587
[3] Sashin V A, Dorsett H E, Bolorizadeh M and Ford M J 2000 *J. Chem. Phys.* **113** 8175
[4] Saunders V R, Dovesi R, Roetti C, Causà M, Harrison N M, Orlando R and Zicovich-Wilson C M 1998 *CRYSTAL98 User's Manual* (Torino: University of Torino)
[5] Dovesi R, Roetti C, Freyria-Fava C and Prencipe M 1991 *Chem. Phys.* **156** 11
[6] Barrie A and Street F J 1975 *J. Electron Spectrosc. Relat. Phenom.* **7** 1
[7] Shek M L, Hrbek J, Sham T K and Xu G Q 1991 *J. Vac. Sci. Technol.* A **9**
[8] Hamalainen K, Huotari S, Laukkanen J, Soininen A, Manninen S, C-Kao C, Buslaps T and Mezouar M 2000 *Phys. Rev.* B **62** R735
[9] Dovesi R, Pisani C, Roetti C, Causà M and Saunders V R 1988 *CRYSTAL88 Program no 577, Quantum Chemistry Program Exchange* (Bloomington, IN: Indiana University)
[10] McCarthy I E and Weigold E 1991 *Rep. Prog. Phys.* **54** 789
Coplan M A, Moore J H and Doering J P 1994 *Rev. Mod. Phys.* **66** 985
[11] Dennison J R and Ritter A L 1996 *J. Electron Spectrosc. Relat. Phenom.* **77** 99
[12] Storer P, Caprari R S, Clark S A, Vos M and Weigold E 1994 *Rev. Sci. Instrum.* **65** 2214
[13] Canney S A, Brunger M J, McCarthy I E, Storer P, Utteridge S, Vos M and Weigold E 1997 *J. Electron Spectrosc. Relat. Phenom.* **83** 65
[14] Fang Z, Guo X, Utteridge S, Canney S A and McCarthy I E 1997 *Rev. Sci. Instrum.* **68** 4396
Utteridge S J, Sashin V A, Canney S A, Ford M J, Fang Z, Oliver D R, Vos M and Weigold E 2000 *Appl. Surf. Sci.* **162/163** 357
[15] Sashin V A, Bolorizadeh M and Ford M J 2001 *Surf. Sci.* **495** 35
[16] Jupille J, Dolle P and Besancon M 1992 *Surf. Sci.* **260** 271
[17] Bertel E, Netzer F P, Rosina G and Saalfeld H 1989 *Phys. Rev.* B **39** 6082
Qiu S L, Lin C L, Chen J and Strongin M 1990 *Phys. Rev.* B **41** 7467
[18] Kittel C 1986 *Introduction to Solid State Physics* (New York: Wiley)
[19] Dirac P A M 1930 *Proc. Camb. Phil. Soc.* **26** 376
[20] Vosko S H, Wilk L and Nusair M 1980 *Can. J. Phys.* **58** 1200
[21] Perdew J P, Burke K and Ernzerhof M 1996 *Phys. Rev. Lett.* **77** 3865
[22] Perdew J P and Ernzerhof M 1996 *J. Chem. Phys.* **105** 9982
Ernzerhof M and Scuseria G E 1999 *J. Chem. Phys.* **110** 5029
[23] Soule de Bas B, Dorsett H E and Ford M J 2003 *J. Phys. Chem. Solids* **64** 495
[24] Sashin V A, Canney S A, Ford M J, Bolorizadeh M, Oliver D R and Kheifets A S 2000 *J. Phys.: Condens. Matter* **12** 125
[25] Kheifets A S, Lower J, Nygaard K J, Utteridge S, Vos M, Weigold E and Ritter A L 1994 *Phys. Rev.* B **49** 2113
[26] Sashin V A, Bolorizadeh M, Kheifets A S and Ford M J 2001 *J. Phys.: Condens. Matter* **13** 4203